PyOxP and PyOxB: the Oxyma-based novel family of phosphonium salts†

Ramon Subirós-Funosas,[a,b] Ayman El-Faham*[a,c,d] and Fernando Albericio*[a,b,e]

Received 12th March 2010, Accepted 19th May 2010
First published as an Advance Article on the web 17th June 2010
DOI: 10.1039/c003719b

Recent studies described the great impact of a non-benzotriazolic family of coupling reagents based on ethyl 2-cyano-2-(hydroxyimino)acetate, Oxyma, as a powerful coupling methodology for peptide synthesis. Here we present the synthesis and evaluation of the derived phosphonium salts *O*-[(1-cyano-2-ethoxy-2-oxoethylidene)amino]-oxytri(pyrrolidin-1-yl) phosphonium hexafluorophosphate (PyOxP) and tetrafluoroborate (PyOxB). Both coupling reagents exhibited higher capacity to suppress racemization in various peptide models and enhanced solubility in DMF and DCM than benzotriazole-based reagents. In addition, the hexafluorophosphate analog PyOxP, combined excellent stability with outstanding efficiency in the assembly of demanding penta and decapeptides that include consecutive Aib residues. Cyclization models revealed the advantages of PyOxP, which rendered a higher percentage of cyclic material than other known potent phosphonium salts.

Introduction

Success in peptide synthesis is highly dependent on the coupling strategy used to form the peptide bond.[1,2] Traditionally, carbodiimides were considered an efficient approach to assemble low to moderate sequences, in consumption with additives (HOBt **1**, HOAt **2** and 6-Cl–HOBt **3**; Fig. 1 left), which lower the likelihood of racemization and other side reactions.[3–5] However, the need for stronger activating reagents led to the introduction of stand-alone onium salts (mainly aminium/uronium and phosphonium ones), which have become the preferred coupling choice in solution- and solid-phase peptide synthesis.[6]

The most powerful onium salts are the aminium/uronium ones. Their structure comprises a carbocation skeleton and an additive, usually benzotriazole-based (HATU **4**, HBTU **5**/TBTU **6**, HCTU **7**/TCTU **8**; Fig. 1 center).[7–9] The tetramethylamino group included in the carbocation skeleton of these classical coupling reagents has recently evolved to a dimethylmorpholino moiety (HDMA **9**, HDMB **10**, 6-Cl–HDMB **11**; Fig. 1 right),[10] thereby resulting in improved stability and solubility in common solvents used in peptide synthesis, as well as an increase in optical purity and reactivity. The high reactivity of both types of aminium/uronium salts may also lead to the appearance of side reactions, usually during slow couplings, such as cyclizations or in the introduction of hindered residues. In these situations, an excess of such a coupling reagent usually causes the attachment of a guanidine moiety to the free N-terminus of the growing peptide chain, thereby blocking any further reaction.[11] Moreover, these reagents are costly for peptide synthesis purposes. Phosphonium salts differ from the former in the nature of the electrophilic core as they have a positively charged phosphorus center and they do not undergo the above mentioned termination of the peptide chain when added in excess. Thus phosphonium salts show similar potency to their aminium/uronium counterparts.[12] These types of onium salts were first introduced by Kenner and coworkers in 1969, although they did not gain general acceptance until the 1990s, when many became commercially available.[13] The most predominant phosphonium salts display a tris(pyrrolidino)phosphonium-type electrophilic core (PyAOP **12**, PyBOP **13**, PyClock, **14**; Fig. 2)[14–16] while their tris(dimethylamino) analogs, of which BOP is the most representative, are slightly less reactive and also originate HMPA as a byproduct, which is a carcinogenic and toxic phosphoramide.[17–19]

In both classes of onium salts, aminium/uronium and phosphonium, the same trend is observed: HOAt (**2**) analogs showed superiority to HOBt (**1**) and 6-Cl–HOBt (**3**) ones in activation and coupling steps and also in reducing the loss of optical purity.[12] In addition, derivatives of 6-Cl–HOBt (**3**) are generally less hazardous and more reactive than HOBt (**1**) counterparts.[9] This relative performance is connected to the acidity of the additive, which is linked to the reactivity of the corresponding active ester. Therefore, PyAOP (**12**) is considered the most reactive phosphonium salt (pK_a of HOAt=3.28), whereas PyClock (**14**) is a good alternative to PyBOP (**13**), because the presence of Cl at position 6 of the benzotriazole ring results in a better leaving group (pK_a of 6-Cl–HOBt=3.35 *vs.* pK_a of HOBt=4.60).[20] However, additional factors contribute to the great difference in reactivity. Thus, it has been proposed that the nitrogen at the 7-position of HOAt creates a neighboring group effect, which results in enhanced reactivity and solubility of its analogs.

[a]*Institute for Research in Biomedicine, Barcelona Science Park, Baldiri Reixac 10, 08028, Barcelona, Spain. E-mail: aymanel_faham@hotmail.com, albericio@irbbarcelona.org; Fax: +34 93-403-71-26; Tel: +34 93-403-70-88*
[b]*CIBER-BBN, Networking Centre on Bioengineering, Biomaterials and Nanomedicine Barcelona Science Park, Baldiri Reixac 10, 08028, Barcelona, Spain*
[c]*Department of Chemistry, College of Science, King Saud University, P.O. Box 2455, Riyadh, 11451, Kingdom of Saudi Arabia*
[d]*Department of Chemistry, Faculty of Science, Alexandria University, Ibrahimia, 21321, Alexandria, Egypt*
[e]*Department of Organic Chemistry, University of Barcelona, Martí i Franqués 1-11, 08028, Barcelona, Spain*

† Electronic supplementary information (ESI) available: ^{1}H and ^{13}C-NMR spectra for PyOxP and PyOxB, and HPLC characterization of racemization and coupling efficiency experiments. See DOI: 10.1039/c003719b

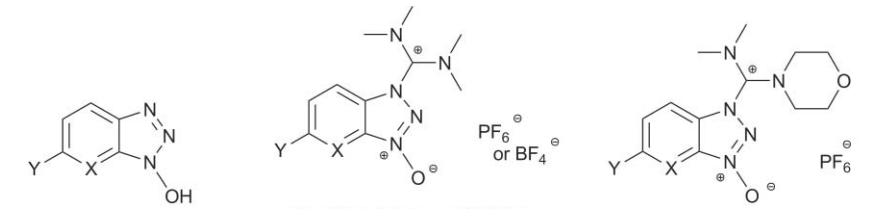

Fig. 1 Benzotriazole-based additives (left), tetramethyl (center) and dimethylmorpholino (right) aminium salts.

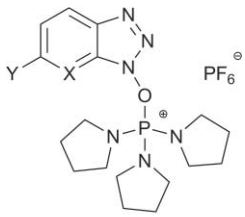

Fig. 2 Benzotriazole-based phosphonium salts.

Recently, we reported ethyl 2-cyano-2-(hydroxyimino)acetate (Oxyma **15**, Fig. 3) and its derived uronium salt 1-[(1-(cyano-2-ethoxy-2-oxoethylideneaminooxy)-dimethylamino-morpholinomethylene)] methanaminium hexafluorophosphate (COMU **16**, Fig. 3) as efficient additive and coupling reagent for peptide synthesis.[21,22] The active esters formed by these reagents are extremely reactive due to the low hindrance and acidity of Oxyma (pK_a = 4.60), which results in an excellent leaving group.[23] Oxyma (**15**) and COMU (**16**) show superiority to HOBt (**1**) derivatives and a similar or even higher potency than HOAt (**2**) analogs in suppressing racemization and assembling demanding peptide models. In terms of safety, **15** and **16** also have a considerably lower risk of explosion than benzotriazole-based reagents and are compatible with microwave irradiation.[24,25]

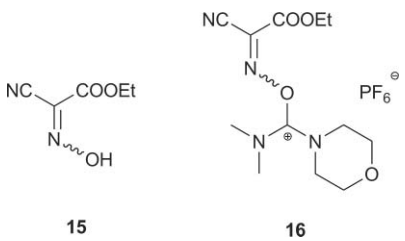

Fig. 3 Oxyma and its derived uronium salt, COMU.

In view of these outstanding results, the next step was to include Oxyma (**15**) in a tris(pyrrolidino)-type phosphonium salt, in both hexafluorophosphate and tetrafluoroborate forms. The synthesis and structure determination of the hexafluorophosphate version was accomplished by Hoffmann *et al.* in 2003, although its suitability as a coupling reagent was not tested.[26] In the present study, we compared the capacity of *O*-[(cyano-(ethoxycarbonyl)methyliden-amino]-yloxytripyrrolidinophosphonium hexafluorophosphate and tetrafluoroborate (PyOxP **17** and PyOxB **18**, Fig. 4) to lower racemization and enhance coupling extension in linear and cyclic peptide models with the abovementioned benzotriazole-based phosphonium salts PyAOP (**12**), PyBOP (**13**) and PyClock (**14**).

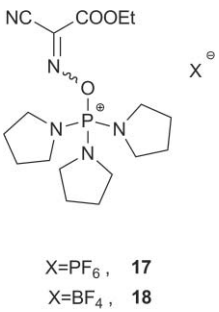

Fig. 4 Structure of the hexafluorophosphate and tetrafluoroborate tris(pyrrolidino)phosphonium salts derived from Oxyma.

Results and discussion

The Oxyma-based phosphonium salts PyOxP (**17**) and PyOxB (**18**) were successfully synthesized in one-pot fashion from Oxyma (**15**) (Scheme 1). The first step consisted of the rapid formation of the intermediate potassium salt of the oxime with potassium carbonate (K_2CO_3) after 10 min of gently stirring. Subsequent addition of PyBroP or the analogous tetrafluoroborate salt to the reaction mixture afforded, after 4 h, the desired phosphonium salts **17** and **18**, in 76% yield after recrystallization from DCM–hexane. Previous formation of the potassium salt is preferred over the addition of a tertiary base to Oxyma (**15**), like Et_3N, to generate the anion, since this method yields $Et_3N^+Br^-$, which is difficult to separate from the desired phosphonium salt.

The stability of phosphonium salts is a basic feature for their optimal performance in peptide synthesis, since they are predominantly used in slow-rate couplings, specially cyclizations, and therefore a rapid hydrolysis of the reagent dramatically decreases their efficiency. In order to check and compare the stability of the proposed oxime-based phosphonium salts with their benzotriazole counterparts, we conducted hydrolysis experiments in an NMR tube (3 days in acetone) and in an open vial (5 days in DMF)

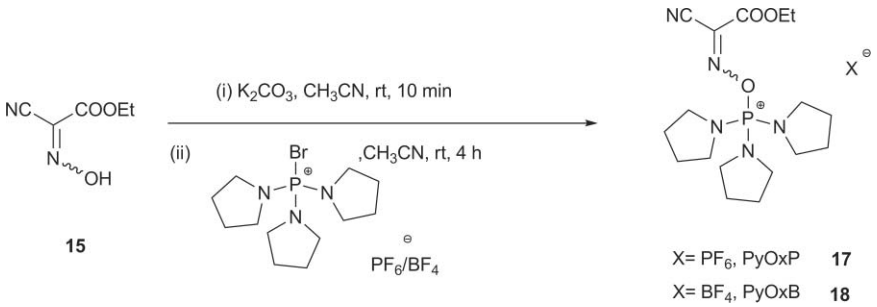

Scheme 1

Table 1 Hydrolytic stability (%) of phosphonium salts during NMR and HPLC assays

Entry	Coupling Reagent	Method of analysis	
		NMR, 3 days (%)[a]	HPLC, 5 h (%)[b]
1	PyAOP (**12**)	10	29
2	PyBOP (**13**)	20	39
3	PyClock (**14**)	50	35
4	PyOxP (**17**)	60	40
5	PyOxB (**18**)	30	25

[a] The samples were dissolved in acetone-d_6 and placed in an NMR tube (closed vial). [b] A solution of the phosphonium salt in DMF was kept at rt in an open vial.

(Table 1). As envisaged, stability in the closed vial was higher than in the open vessel. The hexafluorophosphonium derivative **17** showed slower hydrolysis than its tetrafluoroborate analog **18** in both conditions (entries 4 *vs.* 5). The lower stability of PyOxB (**18**) was evident during the NMR assays, when a freshly prepared solution rapidly changed color (from colorless to yellow in DMF, from yellow to red in DCM), showing 6–7% hydrolysis in NMR. These observations were consistent with the melting points observed for the two Oxyma-based phosphonium salts (131–132 °C for PyOxB *vs.* 185–186 °C for PyOxP). Not only did PyOxP (**17**) show greater stability than PyOxB (**18**), but it was also the most stable phosphonium salt tested, including the benzotriazole analogs PyAOP (**12**), PyBOP (**13**) and PyClock (**14**) (entry 4 *vs.* 1, 2, 3).[12] Amongst these classical reagents, **14** exhibited slower hydrolysis than **12** and a similar rate to **13**, as previously reported (entry 3 *vs.* 1, 2).[16] Finally, in the DMF/DIEA mixture PyOxB (**18**) hydrolyzed the most quickly.

Solubility is also a key feature in determining the suitability of a coupling reagent for peptide synthesis. The solubility of the various phosphonium salts in DMF (generally the solvent of choice in peptide bond formation) and DCM was evaluated (Table 2). All reagents exhibited higher solubility in the more polar solvent (DMF), as expected. The Oxyma derivatives **17** and **18** were considerably more soluble than the benzotriazole ones (**12**, **13**, **14**) in both solvents (entries 4, 5 *vs.* 1, 2, 3). Although displaying lower stability than PyOxP (**17**), PyOxB (**18**) was more soluble, affording up to 3.24 M solutions in DMF (entry 5 *vs.* 4).

Efficient peptide assembly is highly dependent on extension of coupling and yield, but also on the control of optical purity. In order to compare the retention of configuration induced by PyOxP (**17**) and PyOxB (**18**) with that achieved by the benzotriazole-based derivatives **12**, **13** and **14**, three previously studied peptide

Table 2 Solubility of phosphonium salts in DMF and DCM

Entry	Coupling Reagent	DMF		DCM	
		Wt/g mL^{-1}	Molarity	Wt/g mL^{-1}	Molarity
1	PyAOP (**12**)	1.04	1.99	0.92	1.79
2	PyBOP (**13**)	0.80	1.54	0.64	1.23
3	PyClock (**14**)	0.80	1.44	0.40	0.72
4	PyOxP (**17**)	1.36	2.58	1.04	1.97
5	PyOxB (**18**)	1.52	3.24	1.32	2.82

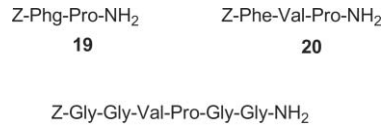

Fig. 5

models were used, which involve stepwise and segment couplings (Fig. 5).[27–29]

The [1+1] stepwise coupling of *Z*-Phg-OH onto H-Pro-NH_2 to afford *Z*-Phg-Pro-NH_2 **19** was performed in the presence of DIEA, in solution and solid phase (Table 3). The Oxyma-based phosphonium salts showed better performance than the benzotriazole-based derivatives in both approaches. The superiority of these

Table 3 Racemization during the [1+1] formation of *Z*-Phg-Pro-NH_2 in DMF (solution and solid-phase synthesis)[a,b,c]

Entry	Coupling approach	Coupling Reagent	DL (%)
1	Solution-phase	PyAOP (**12**)	2.2
2		PyBOP (**13**)	5.8
3		PyClock (**14**)	1.6
4		PyOxP (**17**)	0.3
5		PyOxB (**18**)	0.6
6		PyAOP (**12**)/HOAt (**2**)	2.6
7		PyBOP (**13**)/HOBt (**1**)	5.7
8		PyClock (**14**)/6-Cl-HOBt (**3**)	1.4
9		PyOxP (**17**)/Oxyma (**15**)	0.6
10		PyOxB (**18**)/Oxyma (**15**)	0.6
11	Solid-Phase	PyAOP (**12**)	41.4[d]
12		PyBOP (**13**)	44.2[d]
13		PyClock (**14**)	50.2[d]
14		PyOxP (**17**)	7.4[d]
15		PyOxB (**18**)	10.8[d]

[a] DIEA (2 equiv.) was used as base (for detailed procedure and analysis, see Experimental section).[27] [b] LL and DL forms of the model dipeptide were identified after co-injection with a pure sample of LL. [c] Yields obtained were in the range 88–92%. [d] The percentage in the table is the average of two runs.

Table 4 Racemization during the [2+1] formation of *Z*-Phe-Val-Pro-NH_2 in DMF (solution and solid-phase synthesis) [a,b,c]

Entry	Coupling approach	Coupling Reagent	LDL (%)
1	Solution-phase	PyAOP (**12**)	3.0
2		PyBOP (**13**)	12.5
3		PyClock (**14**)	8.6
4		PyOxP (**17**)	5.7
5		PyOxB (**18**)	5.3
6		PyAOP (**12**)/HOAt (**2**)	1.0
7		PyBOP (**13**)/HOBt (**1**)	8.8
8		PyClock (**14**)/6-Cl-HOBt (**3**)	7.9
9		PyOxP (**17**)/Oxyma (**15**)	3.4
10	Solid-Phase	PyAOP (**12**)	17.3
11		PyBOP (**13**)	29.9
12		PyClock (**14**)	28.6
13		PyOxP (**17**)	23.0
14		PyOxB (**18**)	27.8
15		PyAOP (**12**)/HOAt (**2**)	15.0
16		PyBOP (**13**)/HOBt (**1**)	29.5
17		PyClock (**14**)/6-Cl-HOBt (**3**)	25.2
18		PyOxP (**17**)/Oxyma (**15**)	22.2

[a] TMP (2 equiv.) was used as base (for detailed procedure and analysis, see Experimental section).[27,29] [b] LLL and LDL forms of the model tripeptide were identified after co-injection with a pure sample of LLL. [c] Yields obtained were in the range 88–92%.

salts was greater in the solid-phase synthesis, where racemization with PyOxP (**17**) and PyOxB (**18**) was 4–5 times lower than with PyAOP (**12**), PyBOP (**13**) and PyClock (**14**) (entries 14, 15 *vs.* 11, 12, 13). Among these novel phosphonium salts, **17** afforded the best results regarding optical purity (entries 4, 14 *vs.* 5, 15). In solution, **14** gave lower racemization than **12**, the most potent phosphonium salt known to date (entry 3 *vs.* 1).[16] Addition of the corresponding additive to the onium salt did not have a siginificant effect on the percentage of racemization (entries 6–10 *vs.* 1–5). The performance of the phosphonium salts in stepwise synthesis was also tested in the *Z*-Phe-Ser-Pro-NH_2 model, although this system was not sensitive enough to allow a comparative study (racemization was < 0.1% in all experiments).

The loss of optical purity during the [2+1] segment coupling of dipeptide *Z*-Phe-Val-OH onto H-Pro-NH_2 to yield *Z*-Phe-Val-Pro-NH_2 **20** was higher than in the previous stepwise model. This result is attributed to the greater sensitivity of peptide fragments than single amino acids (Table 4). Given that TMP reduces racemization in segment couplings more efficiently than other bases, its use is recommended in these experiments.[29] Oxyma-based PyOxP (**17**) and PyOxB (**18**) showed a similar performance, giving lower racemizations than HOBt and 6-Cl–HOBt analogs (entries 4, 5 *vs.* 2, 3 and entries 13, 14 *vs.* 11, 12). The addition of additives in peptide model **20** produced a clear increase in the control of optical purity, in contrast to the less sensitive segment coupling **19** (entries 6–9 *vs.* 1–5 and 15–18 *vs.* 10–14).

The retention of configuration in fragment couplings was further tested in the [3+3] formation of the model hexapeptide *Z*-Gly-Gly-Val-Pro-Gly-Gly-NH_2 **21**, a modified version of the well-known system *Z*-Gly-Gly-Val-Ala-Gly-Gly-NH_2, in solid-phase fashion (Table 5).[29] The results indicate the suitability of using the highly hindered base TMP instead of DIEA for segment couplings. Again, Oxyma-based phosphonium salts showed an outstanding performance, regardless of the base used. Of particular note was

Table 5 Yield and racemization during the [3+3] formation of *Z*-Gly-Gly-Val-Pro-Gly-Gly-NH_2 in DMF (solid-phase synthesis)[a,b,c]

Entry	Coupling Reagent	Base (equiv.)	DL (%)
1	PyAOP (**12**)	DIEA (2)	33.7
2	PyBOP (**13**)		51.0
3	PyClock (**14**)		43.1
4	PyOxP (**17**)		22.2
5	PyOxB (**18**)		22.2
6	PyAOP (**12**)	TMP (2)	4.4
7	PyBOP (**13**)		10.2
8	PyClock (**14**)		11.5
9	PyOxP (**17**)		4.1
10	PyOxB (**18**)		6.9

[a] For detailed procedure and analysis see Experimental section. [b] LL and DL forms of the model hexapeptide were identified after co-injection with pure samples. [c] Yields obtained were in the range 88–92%.

the percentage of racemization detected with PyOxP (**17**), which was even lower than that recorded for the HOAt analog **12** (entry 4, 9 *vs.* 1, 6).

After addressing loss of optical purity, the coupling efficiency of PyOxP (**17**), the most stable and strongest racemization-suppressing analog of the Oxyma-based phosphonium salts, was tested in the assembly of complex peptide models, based on Leu-enkephalin pentapeptide (H-Tyr-Gly-Gly-Phe-Leu-NH_2), its linear dimer (H-Tyr-Gly-Gly-Phe-Leu-Tyr-Gly-Gly-Phe-Leu-NH_2) and ACP (65–74) decapeptide (H-Val-Gln-Ala-Ala-Ile-Asp-Tyr-Ile-Asn-Gly-NH_2). The design of the analogs consisted of introducing the hindered α,α-disubstituted amino acid Aib to replace consecutive Gly (Leu-enkephalin and dimer derivatives **22**, **23** and **24**) or Ala (ACP derivative **25**) residues, in order to reduce coupling extension, thereby improving our capacity to distinguish differences between coupling reagents (Fig. 6).

H-Tyr-Aib-Aib-Phe-Leu-NH_2
22

H-Tyr-Aib-Aib-Phe-Leu-Tyr-Gly-Gly-Phe-Leu-NH_2
23

H-Tyr-Gly-Gly-Phe-Leu-Tyr-Aib-Aib-Phe-Leu-NH_2
24

H-Val-Gln-Aib-Aib-Ile-Asp-Tyr-Ile-Asn-Gly-NH_2
25

Fig. 6

Coupling efficiency was first evaluated in the synthesis of the highly demanding Aib-enkephalin analog **22** (H-Tyr-Aib-Aib-Phe-Leu-NH_2).[7a] Coupling times of 30 min, except for the Aib-Aib assembly (30 min double coupling), were applied during solid-phase elongation. The pentapeptide/deletion tetrapeptide ratios obtained with the reagents are given in Table 6. Following the trend observed in the previous experiments, PyOxP (**17**) provided higher yield and extent of coupling than PyAOP (**12**), which was the benzotriazole derivative that best performed, followed by PyClock (**14**) (entry 4 *vs.* 1, 2, 3). The desired pentapeptide was obtained with PyBOP (**13**) in a poor 48.6% yield, in contrast to its Oxyma analog **17**, which afforded near quantitative

Table 6 Percentage of Aib-enkephalin pentapeptide (H-Tyr-Aib-Aib-Phe-Leu-NH_2) and des-Aib deletion tetrapeptide (H-Tyr-Aib-Phe-Leu-NH_2) during solid-phase assembly [a,b]

Entry	Coupling Reagent	Yield (%)	Penta (%)	des-Aib(%)
1	PyAOP (**12**)	89.0	84.8	14.2
2	PyBOP (**13**)	80.2	48.6	47.3
3	PyClock (**14**)	85.0	76.7	23.3
4	PyOxP (**17**)	89.2	98.5	1.5

[a] Couplings were performed with 2 equiv. of DIEA [b] Tetrapeptide (des-Aib) was confirmed by peak overlap in the presence of a true sample (for detailed procedure and analysis, see Experimental section).[7a]

Aib-enkephaline **22**. Thus, **17** showed better performance than its benzotriazole counterparts.

The phosphonium salts were further examined in the elongation of the sterically hindered 8,9- and 3,4-Aib analogs of Leu-enkephaline dimer (**23** and **24**), which displays difficult Leu and Tyr couplings.[30] After short couplings, many nonapeptides (des-Phe, des-Leu, des-Tyr, des-Aib and des-Gly) and octapeptides (des-Aib,Leu, des-Aib,Tyr, des-Leu,Tyr, des-Gly,Tyr and des-Gly,Aib) were produced. The introduction of Aib and the adjacent Tyr was the most demanding coupling (Table 7). The experiments with PyAOP (**12**) resulted in an excellent degree of coupling, although PyOxP (**17**) performed better, affording the target decapeptides in >95% yield (entries 4, 8 *vs.* 1, 5) in solid-phase syntheses. In the benzotriazole series, PyClock (**14**) and PyBOP (**13**) obtained similar percentages of the 8,9-analog **23** (entry 3 *vs.* 2); however, in the synthesis of the 3,4-derivative **24**, PyClock (**14**) showed higher potency than its HOBt counterpart **13** (entry 7 *vs.* 6).

To conclude the coupling efficiency assays, the Aib[67]-Aib[68] modified ACP (64–75) decapeptide (H-Val-Gln-Aib-Aib-Ile-Asp-Tyr-Ile-Asn-Gly-NH_2) **25** was assembled by means of 5 min couplings, except in the formation of Aib-Ile and Aib-Aib peptide bonds (30 min and 30 min double coupling respectively).[31] Misincorporation of one residue (des-Aib, des-Asn, des-Gln and des- Ile[69]) or two (des-Ile[69],Ile[72]) occurred (Table 8). PyOxP (**17**) allowed the introduction of Aib, Asn and Ile[69] to a greater extent than PyAOP (**12**) and PyBOP (**13**), thereby affording 81% of the Aib-decapeptide **25**. In contrast, the benzotriazole counterparts provided only 64% and 48% yield (entry 3 *vs.* 1,2). Higher yield was also obtained with the Oxyma-based phosphonium salt **17** (83.2%).

Finally, the suitability of PyOxP (**17**) and PyOxB (**18**) as coupling reagents in cyclization steps was tested in the synthesis of cyclic Ala-pentapeptide (H-Ala-Ala-*N*MeAla-Ala-Ala-OH).[32,33] The main risk associated with this step is the capping of the N-terminus amino group. This effect has been reported when aminium/uronium salts are used and it leads to guanidylation and termination of the peptide chain (Scheme 2).

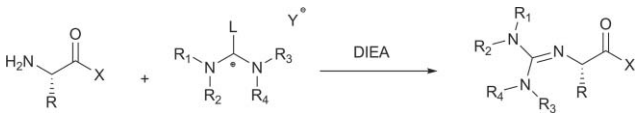

Scheme 2

Once the linear pentapeptide was successfully assembled in solid-phase and cleaved from the resin, a 0.01M solution in DMF was mixed with the corresponding coupling reagent and DIEA. After 24 h, samples were taken and their content was analyzed by reverse-phase HPLC-PDA and HPLC-MS (Table 9).

Table 7 Percentage of 8,9-(H-Tyr-Aib-Aib-Phe-Leu -Tyr-Gly-Gly-Phe-Leu-NH_2) and 3,4-(H-Tyr-Gly-Gly-Phe-Leu-Tyr-Aib-Aib-Phe-Leu-NH_2) Aib-enkephalin decapeptides and deletion peptides during solid-phase assembly[a,b]

Analog	Entry	Coupling Reagent	deca (%)	des-Phe (%)	des-Aib-Leu (%)	des-Aib, Tyr (%)	des-Leu (%)	des- Leu, Tyr (%)	des-Gly, Tyr (%)	des Tyr (%)	des-Aib (%)	des-Gly (%)	des-Gly, Aib (%)
8,9-Aib **23**	1	PyAOP (**12**)	93.3	0.1	—[c]	0.2	0.4	0.2	—[c]	0.9	3.6	1.3	—[c]
	2	PyBOP (**13**)	56.1	0.1	0.3	0.7	0.3	0.2	—[c]	3.4	37.7	1.2	—[c]
	3	PyClock (**14**)	56.2	0.1	0.4	0.1	0.2	0.2	—[c]	2.4	39.1	1.3	—[c]
	4	PyOxP (**17**)	96.5	0.1	—[c]	0.5	0.4	0.2	—[c]	0.1	0.5	1.7	—[c]
3,4-Aib **24**	5	PyAOP (**12**)	85.5	0.3	0.1	0.1	0.3	0.3	0.1	1.2	9.9	1.6	0.6
	6	PyBOP (**13**)	51.5	0.1	0.2	0.3	0.1	0.7	0.1	0.5	44.8	1.2	0.6
	7	PyClock (**14**)	71.5	1.0	0.1	0.1	0.1	0.5	0.1	1.0	24.6	0.8	0.3
	8	PyOxP (**17**)	95.4	0.1	0.1	0.1	0.3	0.7	0.1	1.1	0.5	1.5	0.1

[a] Couplings were performed with 2 equiv. of DIEA (for detailed procedure and analysis, see Experimental section). [b] Apart from the detailed deletion peptides, unknown peaks were observed in all cases at 5.2 and 5.8 min in the 8,9 analog and at 4.6 and 6.6 min in the 3,4-analog (in the range 0.5–3.0%). [c] No misincorporation was detected.

Table 8 Percentage of Aib[67]-Aib[68] analog of ACP (64–75) decapeptide (H-Val-Gln-Aib-Aib-Ile-Asp-Tyr-Ile-Asn-Gly-NH_2) and deletion peptides during solid-phase assembly [a,b]

Entry	Coupling Reagent	Yield (%)	Aib-deca (%)	des-Aib (%)	des-Asn (%)	des-Gln (%)	des-Ile[69], Ile[72] (%)	des-Ile[69] (%)
1	PyAOP (**12**)	81.0	64.0	12.0	3.8	1.0	1.0	10.4
2	PyBOP (**13**)	78.0	48.0	32.0	2.0	0.8	5.0	12.0
3	PyOxP (**17**)	83.2	81.0	2.2	2.2	1.0	1.7	10.1

[a] Fmoc-amino acids were preactivated with coupling reagents in the presence of 1 equiv. of DIEA and then, after addition to the resin, a second equiv. of DIEA was added (for detailed procedure and analysis, see Experimental section). [b] Other unknown peaks were observed, but these were not related to the peptide.

Table 9 Cyclization of H-Ala-Ala-*N*MeAla-Ala-Ala-OH in DMF after 24 h (10^{-2} M).[a,b]

Entry	Coupling Reagent	Cyclic penta (%)	Linear penta (%)	Linear dimer (%)
1	PyAOP (**12**)	54	10	36
2	PyBOP (**13**)	43	28	29
3	PyClock (**14**)	61	15	24
4	PyOxP (**17**)	70	10	20
5	PyOxB (**18**)	47	15	38

[a] The linear pentapeptide was elongated on a 2-chlorotrityl resin by means of DIC/HOAt (**2**)-mediated couplings. [b] 4 equiv. excess of DIEA was used (for detailed procedure and analysis, see Experimental section). [c] In analogous cyclizations performed with HDMA (**9**) and COMU (**16**) in DCM, a high amount of guanidylated material was found (90% and 60% respectively), thus confirming the unsuitability of uronium salts in cyclization steps.

In all experiments, the cyclic product was detected along with the starting linear pentapeptide and the linear dimer. PyOxP (**17**) afforded the highest percentage of cyclized material, closely followed by PyClock (**14**), which showed stronger performance than its HOAt derivative PyAOP (**12**) (entry 4 *vs.* 1, 3). PyBOP (**13**) and PyOxB (**18**) were the least efficient in providing the cyclic pentapeptide, thus confirming the superiority of the hexafluorophosphate version of the Oxyma-based phosphonium salt over the tetrafluoroborate counterpart (entry 4 *vs.* 5).

Conclusions

In summary, PyOxP (**17**) and PyOxB (**18**), the hexaflurophosphate and tetrafluoroborate phosphonium salts derived from Oxyma (**15**), have been successfully obtained in a one-pot procedure from ethyl 2-cyano-2-(hydroxyimino)acetate. This was achieved through reaction of the intermediate potassium salt and PyBroP or its analogous tetrafluoroborate salt to afford the reagents in good yields and high purities. The presence of Oxyma (**15**) conferred the reagents higher solubility in standard solvents for peptide synthesis than PyAOP (**12**), PyBOP (**13**) and PyClock (**14**). Consistently, the analysis of racemization models, involving either [1+1] stepwise or [2+1] and [3+3] segment couplings, showed a higher control of optical purity of PyOxP (**17**) and PyOxB (**18**) over their HOBt and 6-Cl–HOBt counterparts, and similar performance to that of the HOAt derivative.

Although PyOxP (**17**) and PyOxB (**18**) allow the preparation of more concentrated solutions, the use of the former is preferred in view of its higher stability and coupling efficiency, both in the assembly of linear and cyclic peptide models. Apart from being more stable in solution than PyAOP (**12**), PyBOP (**13**) and PyClock (**14**), PyOxP (**17**) also showed greater coupling performance during the elongation of the sterically demanding Leu-enkephalin and ACP (64–75) derivatives that present consecutive Aib residues. With respect to the cyclization of H-Ala-Ala-NMeAla-Ala-Ala-OH, PyOxP (**17**) afforded the cyclized product in the highest percentage, superior to that achieved in the synthesis with PyAOP and with a lower percentage of the linear by-products.

In conclusion, PyOxP (**17**) showed superiority not only over PyBOP (**13**) and PyClock (**14**), but also over PyAOP (**12**), the most potent phosphonium salt known to date. Moreover, given its high stability in open and closed vials, the use of PyOxP is advantageous and highly recommended in automated peptide synthesizers.

Experimental

Materials

The solvents used were of HPLC reagent grade. Oxyma Pure was obtained from Luxembourg Biotechnologies. Melting points were measured in open capillary tubes with a Buchi B-540 melting point apparatus and were uncorrected. ^{1}H NMR and ^{13}C NMR magnetic resonance spectra were recorded on a Varian Mercury 400 MHz spectrometer at rt with chemical shift values reported in δ units (ppm) relative to tetramethylsilane (TMS) as internal standard. For analytical separation and characterization, a reverse-phase Waters 2695 HPLC separation module, coupled to a Waters 2998 PDA UV detector, was used. Chromatograms were processed with Empower software. Peptide mass was detected by means of an HPLC-PDA system as described above, coupled to a Waters Micromass ZQ mass detector, using the MassLynx 4.1 software. Elemental analyses were performed on a Perkin-Elmer 2400 elemental analyzer, and the values found were within ±0.3% of the theoretical values. Follow-up of the synthesis of the phosphonium salts was done by TLC on silica gel-protected aluminium sheets (Type 60 GF254, Merck) and the spots were detected by exposure to UV-lamp at λ 254 nm for a few seconds. The compounds were named using ChemBioDraw Ultra version 12.0, Cambridge soft Corporation. Samples were introduced into a Waters Synapt HDMS mass spectrometer by direct infusion and exact masses were determined (ESI positive polarity, W analyzer, 3000 V capillary voltage, 150 °C and 100 °C desolvation and source temperature, 40 V sample cone, 100–1500 m/z).

One-pot synthesis of PyOxP (17) and PyOxB (18)

Oxyma (20 mmol; 2.84 g) was suspended in ACN (50 mL) and potassium carbonate (10 mmol; 1.38 g) was added. The reaction mixture was stirred at rt for 10 min and then 20 mmol of the bromophosphonium salt (PyBroP or its tetrafluoroborate analog) was added under nitrogen atmosphere. The reaction mixture was stirred at rt for 4 h, filtered from the precipitate and washed with ACN (10 mL). The filtrate was concentrated under vacuum and diethylether was added with stirring to provide the phosphonium salts in 76% yield (7.9 g), after recrystallization from DCM–hexane. PyOxP: mp = 185–186 °C; ^{1}H NMR ($CDCl_3$): δ 1.41 (t, 3H, CH_3), 2.01–2.04 (m, 12H, 6 C-CH_2), 3.37–3.41 (m, 12H, 6 N-CH_2), 4.47 (q, 2H, CH_2) ppm; ^{13}C NMR ($CDCl_3$):δ 14.00, 26.39, 48.29, 65.07, 106.31, 135.80, 135.95, 155.87 ppm.; elemental analysis (%) calculated for $C_{17}H_{29}F_6N_5O_3P_2$ (527.38): C, 38.72; H, 5.54; F, 21.61; N, 13.28. Found: C, 38.59; H, 5.45; N, 13.38. PyOxB: mp = 131–132 °C; H^{1} NMR (acetone-d_6): δ 1.36 (t, 3H, CH_3), 2.04–2.05 (m, 12H, 6 C-CH_2), 3.51–3.53 (m, 12H, 6 N-CH_2), 4.45 (q, 2H, CH_2) ppm,^{13}C NMR (acetone-d_6):δ 13.47, 26.21, 47.97, 64.28, 106.97, 136.69, 136.84, 156.36 ppm. A sample for exact mass determination was prepared, dissolving in CH_3CN and diluting 1 to 100 in H_2O–CH_3CN (1 : 1): $[M]^+$=382.2009. PyOxP and PyOxB were also characterized by HPLC, using a Sun fire C_{18} (3.5 µm, 4.6 × 100 mm) column, linear gradient 5 to 100% of 0.036% TFA in CH_3CN/0.045%TFA in H_2O over 8 min; flow rate = 1.0 ml min^{-1}; detection at 220 nm; t_R (PyOxP)= 5.19 min, t_R (PyOxB) = 5.17 min.

Racemization tests using model peptides in solution and solid phase[27,29]

Solution-phase tests were conducted adding the coupling reagent (0.125 mmol, 1 equiv.) to a solution of the amino acids (1 equiv. each) in DMF (1 mL) in the presence of base (2 equiv.) at 0 °C. The resulting mixture was stirred for 3–4 h in an ice bath. The work-up of the reaction mixture was as previously described for *Z*-Phg-Pro-NH_2 and *Z*-Phe-Val-Pro-NH_2.[27] For solid-phase assays, the coupling was performed with H-Pro-RinkAmide-PS-resin or H-Pro-Gly-Gly-RinkAmide-PS-resin, 3 equiv. of the corresponding acid (*Z*-Phg-OH, *Z*-Phe-Val-OH or *Z*-Gly-Gly-Val-OH) and 3 equiv. of the corresponding coupling reagent in DMF at rt, with preactivation of 10–30 s with 6 equiv. of base (DIEA or TMP).[22] The reaction mixture was left 3–4 h at rt. The peptide was recovered after cleavage from the resin with 50% TFA in DCM for 1 h at rt. TFA and DCM were removed *in vacuo* and the crude peptide was precipitated with ether or dissolved in ACN and injected directly into the HPLC apparatus. Crude products from the solution- and solid-phase tests were analyzed by reverse-phase HPLC-PDA, using a Sun fire C_{18} (3.5 μm, 4.6 × 100 mm) column, linear gradient of 20 to 50% (*Z*-Phg-Pro-NH_2) over 20 min, linear gradient of 20 to 70% (*Z*-Phe-Val-Pro-NH_2) over 8 min or linear gradient of 10% to 60% (*Z*-Gly-Gly-Val-Pro-Gly-Gly-NH_2) CH_3CN/0.036% TFA in H_2O/0.045% TFA over 8 min; flow = 1.0 mL min^{-1} detection at 220 nm. t_R (*Z*-L-Phg-Pro-NH_2) = 12.51 min, t_R (*Z*-D-Phg-Pro-NH_2) = 13.07 min, t_R (*Z*-Phe-L-Val-Pro-NH_2) = 6.95 min, t_R (*Z*-Phe-D-Val-Pro-NH_2) = 7.43 min, t_R (*Z*-Gly-Gly-L-Val-Pro-Gly-Gly-NH_2) = 5.53 min, t_R (*Z*-Gly-Gly-D-Val-Pro-Gly-Gly-NH_2) = 5.91 min.

Solid-phase synthesis of Aib-enkephalin pentapeptide (H-Tyr-Aib-Aib-Phe-Leu-NH_2)[7a]

The synthesis was carried out in a plastic syringe attached to a vacuum manifold so as to effect rapid removal of reagents and solvent. The Fmoc-RinkAmide-AM-PS (loading = 0.63 mmol g^{-1}, 100 mg) resin was swelled in DCM and conditioned in DMF (2 × 10 mL each). The resin was deblocked by treatment with 20% piperidine in DMF (10 mL) for 10 min. The resin was washed with DMF, DCM and DMF (2 × 10 mL each) and then acylated with a solution of Fmoc-Leu-OH (3 equiv.) and coupling reagent (3 equiv.) in 0.4 mL of DMF, previously preactivated with DIEA (6 equiv.) for 1–2 min before addition to the resin. The reaction mixture was stirred slowly for 1 min and allowed to couple for 30 min (30 min double coupling for Aib-Aib peptide bond formation). The resin was washed with DMF, and then deblocked by treatment with 20% piperidine in DMF for 7 min. The resin was washed with DMF, DCM and DMF (2 × 10 mL each) and then coupled with the next amino acid to obtain the pentapeptide. The peptide was cleaved from the resin after treatment with TFA–H_2O (9 : 1) at rt for 2 h. TFA was removed *in vacuo* and the crude peptide was precipitated with diethyl ether. The weight of the crude product was recorded and purity was determined by reverse-phase HPLC-PDA, using a Sun fire C_{18} (3.5 μm, 4.6 × 100 mm) column, linear gradient 0 to 100% of 0.036% TFA in CH_3CN/0.045%TFA in H_2O over 15 min; flow rate = 1.0 ml min^{-1}; detection at 220 nm; t_R (penta) = 6.68 min, $[M+H]^+$=611.0; t_R (des-Aib) = 6.78 min, $[M+H]^+$=526.4. Neither des-Tyr (448.3) nor tripeptide (363.5) were observed.

Solid-Phase Synthesis of Aib-ACP (65–74) decapeptide (H-Val-Gln-Aib[67]-Aib[68]-Ile[69]-Asp-Tyr-Ile[72]-Asn-Gly-NH_2)[31]

The synthesis was conducted in a plastic syringe attached to a vacuum manifold so as to effect rapid removal of reagents and solvent. The Fmoc-RinkAmide-MBHA-PS resin (loading = 0.45 mmol g^{-1}, 100 mg) was swelled in DCM and conditioned in DMF (2 × 10 mL each). The Fmoc-protecting group was removed by treatment with 20% piperidine in DMF (10 mL) for 10 min, and the resin was washed with DMF, DCM and DMF (2 × 10 mL each). Acylation took place by mixing the resin with a solution of Fmoc-Gly-OH (3 equiv.), and coupling reagent (2 equiv.) in 0.4 mL DMF, previously preactivated with DIEA (2 equiv.) for 1–2 min, followed by addition of extra 2 equiv. of DIEA. The reaction mixture was stirred slowly for 1 min and allowed to couple for 5 min (30 min coupling for Aib-Ile and 30 min double coupling in case of Aib-Aib). The resin was washed with DMF, and then deblocked with a solution of 20% piperidine in DMF for 7 min. The resin was washed with DMF, DCM, DMF (2 × 10 mL each) and then coupled with the next amino acid to obtain the pentapeptide. The peptide was cleaved from the resin by treatment with TFA–H_2O (9 : 1) at rt for 2 h. TFA was removed *in vacuo* and the crude peptide was precipitated with ether. The precipitate was then redissolved in H_2O and lyophilized. The weight of the crude product was recorded and the purity was determined by HPLC analysis, using a Sun fire C_{18} (3.5 μm, 4.6 × 100 mm) column, linear gradient 10 to 35% of 0.036% TFA in CH_3CN/0.045%TFA in H_2O over 8 min; flow rate = 1.0 ml min^{-1}; detection at 220 nm; t_R (Aib-ACP) = 6.41 min, $[M+H]^+$=1091.2; t_R (des-Aib) = 6.57 min, $[M+H]^+$ = 1005.1; t_R (des-Asn) = 6.67 min, $[M+H]^+$ = 997.2; t_R (des-Gln) = 6.95 min, $[M+H]^+$ = 963.4; t_R (des-Ile[69], Ile[72]) = 5.12 min, $[M+H]^+$= 863.9; t_R (des-Ile[69]) = 6.22 min, $[M+H]^+$= 976.5.

Solid-phase synthesis of 8,9-Aib enkephalin decapeptide (H-Tyr-Aib-Aib-Phe-Leu-Tyr-Gly-Gly-Phe-Leu-NH_2)[30]

The synthesis was carried out in a plastic syringe attached to a vacuum manifold so as to effect rapid removal of reagents and solvent. The resin Fmoc-Rink-amide-AM-PS (loading = 0.63 mmol g^{-1}, 100 mg) resin was swelled in DCM and conditioned in DMF (2 × 10 mL each). The resin was deblocked by treatment with 20% piperidine in DMF (10 mL) for 10 min. The resin was washed with DMF, DCM and DMF (2 × 10 mL each) and then acylated with a solution of Fmoc-Leu-OH (3 equiv.) and coupling reagent (3 equiv in 0.4 mL of DMF, previously preactivated with DIEA (6 equiv.) for 1–2 min before addition to the resin. The reaction mixture was stirred slowly for 1 min and allowed to couple for 30 min (30 min double coupling for Aib-Aib coupling). The resin was washed with DMF and then deblocked by treatment with 20% piperidine in DMF for 7 min. The resin was washed with DMF, DCM and DMF (2 × 10 mL each) and then coupled with the next amino acid to obtain the pentapeptide. The peptide was cleaved from the resin after treatment with TFA–H_2O (9 : 1) at rt for 2 h. TFA was removed *in vacuo* and the crude peptide was precipitated with diethyl ether. The weight of the crude product was recorded and purity was determined by reverse-phase HPLC-PDA, using a XBridge C_{18} (2.5 μm, 4.6 × 75 mm) column, linear gradient 30 to 37% of 0.036% TFA in CH_3CN/0.045%TFA in H_2O

over 8 min; flow rate = 1.0 ml min^{-1}; detection at 220 nm; t_R (des-Phe) = 3.31 min, $[M+H]^+$ = 1001.5; t_R (des-Aib,Tyr) = 3.65 min, $[M+H]^+$ = 900.6; t_R (des-Leu) = 3.74 min, $[M+H]^+$ = 1035.5; t_R (des-Leu,Tyr) = 4.26 min, $[M+H]^+$ = 872.5; t_R (des-Aib,Leu) = 4.40 min, $[M+H]^+$ = 950.5; t_R (des-Tyr) = 4.82 min, $[M+H]^+$ = 985.7; t_R (decapeptide) = 6.17 min, $[M+H]^+$ = 1148.7; t_R (des-Aib) = 6.73 min, $[M+H]^+$ = 1063.6; t_R (des-Gly) = 8.11 min, $[M+H]^+$ = 1091.6.

Solid-phase synthesis of 3,4-Aib enkephalin decapeptide (H-Tyr-Gly-Gly-Phe-Leu-Tyr-Aib-Aib-Phe-Leu-NH_2)[30]

The synthesis was carried out in a plastic syringe attached to a vacuum manifold so as to effect rapid removal of reagents and solvent. The resin Fmoc-Rink-amide-AM-PS (loading = 0.63 mmol g^{-1}, 100 mg) resin was swelled in DCM and conditioned in DMF (2 × 10 mL each). The resin was deblocked by treatment with 20% piperidine in DMF (10 mL) for 10 min. The resin was washed with DMF, DCM and DMF (2 × 10 mL each) and then acylated with a solution of Fmoc-Leu-OH (3 equiv.) and coupling reagent (3 equiv.) in 0.4 mL of DMF, previously preactivated with DIEA (6 equiv.) for 1–2 min before addition to the resin. The reaction mixture was stirred slowly for 1 min and allowed to couple for 30 min (only 10 min for the last five residues). The resin was washed with DMF and then deblocked by treatment with 20% piperidine in DMF for 7 min. The resin was washed with DMF, DCM, DMF (2 × 10 mL each) and the coupling and deblocking cycles were repeated to obtain the decapeptide. The peptide was cleaved from the resin after treatment with TFA–H_2O (9 : 1) at rt for 2 h. TFA was removed *in vacuo* and the crude peptide was precipitated with diethyl ether. The weight of the crude product was recorded and purity was determined by reverse-phase HPLC-PDA, using a XBridge C_{18} (2.5 μm, 4.6 × 75 mm) column, linear gradient 32 to 35% of 0.036% TFA in CH_3CN/0.045%TFA in H_2O over 8 min; flow rate = 1.0 ml min^{-1}; detection at 220 nm; t_R (des-Phe) = 3.43 min, $[M+H]^+$ = 1001.4; t_R (des-Aib,Leu) = 3.71 min, $[M+H]^+$ = 950.6; t_R (des-Leu) = 4.27 min, $[M+H]^+$ = 1035.5; t_R (des-Leu,Tyr) = 4.81 min, $[M+H]^+$ = 872.5; t_R (des-Gly,Tyr) = 5.69 min, $[M+H]^+$ = 928.7; t_R (des-Tyr) = 5.90 min, $[M+H]^+$ = 985.8; t_R (des-Aib,Tyr) = 6.24 min, $[M+H]^+$ = 950.5; t_R (decapeptide) = 7.54 min, $[M+H]^+$ = 1148.7; t_R (des-Aib) = 8.21 min, $[M+H]^+$ = 1063.7; t_R (des-Gly) = 8.53 min, $[M+H]^+$ = 1091.8; t_R (des-Gly,Aib) = 9.04 min, $[M+H]^+$ = 1006.8

Synthesis and cyclization of H-Ala-Ala-NMeAla-Ala-Ala-OH.[32,33]

A: Solid-phase synthesis.[32]. The synthesis was conducted in a plastic syringe attached to a vacuum manifold in order to effect rapid removal of reagents and solvent. The 2-chlorotritylchloride resin (loading = 1.55 mmol g^{-1}; 1 g) was swelled in DCM (3 × 50 mL), and then acylated with Fmoc-Ala-OH (2 mmol) and DIEA (14 mmol) in 10 mL of DCM. The reaction mixture was stirred slowly for 1 min and allowed to couple for 15 min. Then, an extra 6 mmol of DIEA was added and the resin was left to stand with stirring from time to time for 45 min. 1 mL of MeOH was added to the resin, stirred for 5 min and allowed to stand for an additional 5 min. The resin was filtered and then washed with DCM and DMF (2 × 50 mL each). Deblocking of the N-terminus was accomplished with 20% piperidine in DMF for 7 min. The resin was washed with DMF, DCM, and DMF (2 × 50 mL each) and then coupled with the next Fmoc-Ala-OH (3 mmol) by means of DIC (3 mmol), and HOAt (3 mmol) for 1 h (1 h double coupling for the coupling of Fmoc-Ala-OH with H-NMeAla-Ala-Ala-Resin). The coupling and deblocking cycles were repeated to obtain the pentapeptide. The peptide was cleaved from the resin by treatment with 50 mL of TFA/DCM (2%) at rt for 5 min. The resin was filtered and then washed with an extra solution of 2% in TFA/DCM (20 mL). TFA and DCM were removed *in vacuo* and the crude peptide was precipitated with cold diethyl ether. The precipitate was then collected and washed two extra times. After drying the peptide under vacuum (1.0 g, 66.5% yield), purity (99.0%) was determined by reverse-phase HPLC analysis using a Sun fire C_{18} (3.5 μm, 4.6 × 100 mm) column, linear gradient 5 to 25% of 0.036% TFA in CH_3CN/0.045%TFA in H_2O over 8 min; flow rate = 1.0 ml min^{-1}; detection at 220 nm; t_R (penta Ala) = 2.99 min, $[M+H]^+$ = 388.2.

B: Cyclization. The cyclization step was performed as reported in a previous study.[32] The linear pentapeptide (0.1 mmol) was cyclized by treatment with the corresponding coupling reagent (0.11 mmol) and 0.44 mmol of DIEA in DMF (10 mL, 0.01 M). After removing DMF under reduced pressure, the crude product was extracted with methanol and precipitated with ether. The sample was dissolved with 100 μl of 1%TFA/H_2O, completing the volume to 1 ml with ACN. 10 μl of the resulting solution was injected into a reverse-phase HPLC apparatus using a Sun fire C18 (3.5 μm, 4.6 × 100 mm) column, linear gradient 5 to 55% of 0.036% TFA in CH_3CN/0.045%TFA in H2O over 8 min; flow rate = 1.0 ml min^{-1}; detection at 220 nm; t_R (linear pentapeptide) = 2.65 min, $[M+H]^+$ = 388.2; t_R (cyclic pentapeptide)= 7.12 min, $[M+H]^+$ = 370.7; t_R (linear dimer) = 8.67 min, $[M+H]^+$ = 739.5.

Acknowledgements

This work was partially supported by CICYT (CTQ2006-03794/BQU), Luxembourg Bio Technologies, Ltd. (Rehovot), the *Generalitat de Catalunya* (2005SGR 00662), the Institute for Research in Biomedicine, and the Barcelona Science Park. RS-F thanks the *Ministerio de Educación y Ciencia* for a FPU PhD fellowship.

Notes and references

1 Abbreviations not defined in text: Aib, α-aminoisobutyric acid; ACN, CH_3CN, ACP, acyl carrier protein decapeptide (65–74); AM-PS, aminomethyl-polystyrene resin; DIC, *N*,*N*′-diisopropylcarbodiimide; BOP, benzotriazol-1-yloxytris(dimethylamino)phosphonium hexafluorophosphate; COMU, 1-[(1-(cyano-2-ethoxy-2-oxoethylideneaminooxy)-dimethylamino-morpholinomethylene)] methanaminium hexafluorophosphate DCM, dicloromethane; DIEA, *N*,*N*-diisopropylethylamine; DMF, *N*,*N*-dimethylformamide; HOBt, 1-hydroxybenzotriazole; 6-Cl-HOBt, 6-chloro-1-hydroxybenzotriazole; HOAt, 7-aza-1-hydroxybenzotriazole; HATU, *N*-[(dimethylamino)-1*H*-1,2,3-triazolo[4,5-*b*]pyridin-1-yl-methylene)-*N*-methylmethanaminium hexafluorophosphate *N*-oxide; HBTU, *N*-[(1*H*-benzotriazol-1-yl)-(dimethylamino)methylene]*N*-methylmethanaminium hexafluorophosphate *N*-oxide; HCTU, *N*-[(6-chloro-1*H*-benzotriazol-1-yl)-(dimethylamino)methylene]*N*-methylmethanaminium hexafluorophosphate *N*-oxide; HDMA, 1-((dimethylimino)(morpholino)-methyl)3-*H*-[1,2,3]triazolo[4,5-*b*]pyridine-1-3-olate hexafluorophosphate; HDMB, 1-((dimethylimino)(morpholino)methyl)3-*H*-benzo-[1,2,3]triazolo-1-ium-3-olate hexafluorophosphate; 6-Cl-HDMB,

1-((dimethylimino)(morpholino)methyl)3-*H*-6-chlorobenzo[1,2,3]triazolo-1-ium-3-olate hexafluorophosphate; MBHA-PS, 4-methylbenzhydrylamine resin; Oxyma, ethyl 2-cyano-2-(hydroxyimino) acetate; Phg, α-phenylglycine; PyAOP, azabenzotriazol-1-yl-*N*-oxy-tris(pyrrolidino)phosphonium hexafluorophosphate; PyBOP, benzotriazol-1-yl-*N*-oxy-tris(pyrrolidino)phosphonium hexafluorophosphate; PyClock, 6-chloro-benzotriazol-1-yl-*N*-oxy-tris-pyrrolidino-phosphonium hexafluorophosphate; PyOxB, *O*-[(1-cyano-2-ethoxy-2-oxoethylidene)amino]-oxytri(pyrrolidin-1-yl) phosphonium tetrafluoroborate; PyOxP, *O*-[(1-cyano-2-ethoxy-2-oxoethylidene)amino]-oxytri(pyrrolidin-1-yl) phosphonium hexafluorophosphate TBTU, *N*-[(1*H*-benzotriazol-1-yl)-(dimethylamino)methylene]*N*-methylmethanaminium tetrafluoroborate *N*-oxide; TCTU, *N*-[(6-chloro-1*H*-benzotriazol-1-yl)-(dimethylamino)methylene]*N*-methylmethanaminium tetrafluoroborate *N*-oxide; TFA, trifluoroacetic acid; TMP, 2,4,6-trimethylpyridine (collidine); Z, benzyloxycarbonyl; Amino acids and peptides are abbreviated and designated following the rules of the IUPAC-IUB Commission of Biochemical Nomenclature [*J. Biol. Chem.*, 1972, **247**(4), 977–983].

2 S.-Y. Han and Y.-A. Kim, *Tetrahedron*, 2004, **60**, 2447–2467.
3 L. A. Carpino, *J. Am. Chem. Soc.*, 1993, **115**, 4397–4398.
4 M. Ueki, T. Yanagihara, Peptides 1998, *25th Proceedings of the European Peptide Symposium*, S. Bajusz, F. Hudecz, Eds, Akademiai Kiado, Budapest, 1999, 252-253.
5 D. H. Rich and J. Singh, *Peptides*, 1979, **1**, 241–261.
6 F. Albericio, R. Chinchilla, D. Dodsworth and C. Nájera, *Org. Prep. Proced. Int.*, 2001, **33**, 203–303.
7 L. A. Carpino, A. El-Faham, C. A. Minor and F. Albericio, *J. Chem. Soc., Chem. Commun.*, 1994, 201–203; L. A. Carpino, H. Imazumi, A. El-Faham, F. J. Ferrer, C. Zhang, Y. Lee, B. M. Foxman, P. Henklein, C. Hanay, C. Mügge, H. Wenschuh, J. Klose, M. Beyermann and M. Bienert, *Angew. Chem., Int. Ed.*, 2002, **41**, 441–445.
8 V. Dourtoglou, J.-C. Ziegler and B. Gross, *Tetrahedron Lett.*, 1978, **19**, 1269–1272; R. Knorr, A. Trzeciak, W. Bannwarth and D. Gillessen, *Tetrahedron Lett.*, 1989, **30**, 1927–1930.
9 O. Marder, Y. Shvo and F. Albericio, *Chimica Oggi*, 2002, **20**(7/8), 37–41.
10 A El-Faham and F. Albericio, *Org. Lett.*, 2007, **9**, 4475–4477; A. El-Faham and F. Albericio, *J. Org. Chem.*, 2008, **73**, 2731–2737.
11 H. Gausepohl, U. Pieles, R. W. Frank, *Peptides-Chemistry and Biology: Proceedings of the 12th American Peptide Symposium*J. A. Smith, J. E. Rivier. Eds; ESCOM, Science: Leiden, 1992, 523-524; S. C. Story and J. V. Aldrich, *Int. J. Pept. Protein Res*, 1994, **43**, 292–296; S. Arttamangkul, B. Arbogast, D. Barofsky and J. V. Aldrich, *Lett. Pept. Sci.*, 1996, **3**, 357–370.
12 F. Albericio, J. M. Bofill, A. El-Faham and S. A. Kates, *J. Org. Chem.*, 1998, **63**, 9678–9683.
13 G. Gawne, G. W. Kenner and R. C. Sheppard, *J. Am. Chem. Soc.*, 1969, **91**(20), 5669–5671.
14 F. Albericio, M. Cases, J. Alsina, S. A. Triolo, L. A. Carpino and S. A. Kates, *Tetrahedron Lett.*, 1997, **38**(27), 4853–4856.
15 J. Coste, D. Le-Nguyen and B. Castro, *Tetrahedron Lett.*, 1990, **31**(2), 205–208.
16 R. Subirós-Funosas, J. A. Moreno, N. Bayó-Puxan, K. Abu-Rabeah, A. Ewenson, D. Atias, R. S. Marks and F. Albericio, *Chimica Oggi*, 2008, **26**(4), 10–12.
17 B. Castro, J. R. Dormoy, G. Evin and C. Selve, *Tetrahedron Lett.*, 1975, **16**, 1219–1222.
18 B. Castro, J. R. Dormoy, B. Dourtoglou, G. Evin, C. Selve and J. C. Ziegler, *Synthesis*, 1976, 751–752.
19 R. R. Dykstra, *Encyclopedia of Reagents for Organic Synthesis*, Vol. 4L. A. Paquette, Ed. John Wiley & Sons Ltd.: Chichester, U.K., 2001, 2668.
20 Y. Azev, G. A. Mokrushina, I. Y. Postovoskii, I. Y. N. Sheinker and O. S. Anisimova, *Chem. Heterocycl. Compd.*, 1976, **12**, 1172–1176; O. Marder and F. Albericio, *Chimica Oggi*, 2003, **21**(6), 35–40.
21 R. Subirós-Funosas, R. Prohens, R. Barbas, A. El-Faham and F. Albericio, *Chem.–Eur. J.*, 2009, **15**, 9394–9403.
22 A. El-Faham, R. Subirós-Funosas, R. Prohens and F. Albericio, *Chem.–Eur. J.*, 2009, **15**, 9404–9416.
23 M. Itoh, *Bull. Chem. Soc. Jpn.*, 1973, **46**(7), 2219–2221; J. Izdebski, *Pol. J. Chem.*, 1979, **53**(5), 1049–1057.
24 K. D. Wehrstedt, P. A. Wandrey and D. Heitkamp, *J. Hazard. Mater.*, 2005, **126**, 1–7.
25 R. Subirós-Funosas, G. A. Acosta, A. El-Faham and F. Albericio, *Tetrahedron Lett.*, 2009, **50**(45), 6200–6202.
26 F. Hoffmann, L. Jaeger and C. Griehl, *Phosphorus, Sulfur Silicon Relat. Elem.*, 2003, **178**(2), 299–309.
27 L. A. Carpino, A. El-Faham and F. Albericio, *J. Org. Chem.*, 1995, **60**, 3561–3564.
28 H. Wenschuh, M. Beyermann, H. Haber, J. K. Seydel, E. Krause, M. Bienert, L. A. Carpino, A. El-Faham and F. Albericio, *J. Org. Chem.*, 1995, **60**, 405–410.
29 L. A. Carpino and A. El-Faham, *J. Org. Chem.*, 1994, **59**, 695–698.
30 J. Hachmann and M. Lebl, *Biopolymers*, 2006, **84**, 340–347.
31 L. A. Carpino, D. Ionescu, A. El-Faham, M. Beyermann, P. Henklein, C. Hana, H. Wenschuh and M. Bienert, *Org. Lett.*, 2003, **5**, 975–977.
32 J. Klose, A. El-Faham, P. Heinklein, L. A. Carpino and M. Bienert, *Tetrahedron Lett.*, 1999, **40**, 2045–2048.
33 A. Ehrlich, U. Heyne, R. Winter, M. Beyermann, H. Haber, L. A. Carpino and M. Bienert, *J. Org. Chem.*, 1996, **61**, 8831–8838.